

Comparison of vegetation indices obtained by drone and satellite

Balázs Gati^{1*}

¹University of Nyiregyhaza, Institute of Technical and Agricultural Sciences, 4400 Nyiregyhaza, Sóstói út 31/B, Hungary

Abstract. Monitoring a crop field with high spatial and temporal resolution with traditional methods is a time and resource consuming activity. Multispectral drone and Sentinel 2 imagery were performed with a temporal resolution of appx. one week in a time frame of 69 days before harvesting in case of a triticale field in Central-Europe subject of organic farming. Results show impressive correlation in the chosen vegetation index (NDVI) in the last month before harvesting. Spatial correlation seems to be a function of the soil characteristic.

1 Introduction

Remote sensing is a developing technology to provide detailed georeferenced information on the Earth's surface [1]. Monitoring crop fields especially biochemical and biophysical traits of crop with several meter or submeter level spatial resolution is essential for precision farming to acquire information about crop stresses, nutrient status, and yield prediction [2]. The traditional field management uses lab-based analysis of direct (manually or automated) acquired soil and crop samples [3]. This method requires significant amount of human and financial resources and results in low spatial resolution, thus not feasible in large scales. However, remote sensing technologies seem to be a promising way to acquire the demanded information, thus intensive research and development aim finding optimal solutions [4,5]. The two well-known ways for remote sensing are the satellites and unmanned aerial systems, such multicopters or drones for short. Multispectral cameras can be installed on both platforms. Satellite images can be accessed by several service providers, even free of charge, such the Sentinel-2 imagery from the Copernicus project founded by the European Union [6], which spectral bands were optimized for crop monitoring [7]. Drones were introduced by innovative researcher and spinoffs [8]. The possibility to establish a complete software and hardware system based mainly on open-source and open-hardware items still exists, but today drone imagery is supported also by commercial user-friendly software and hardware, or can be obtained from service providers, too.

* Corresponding author: gati.balazs@nye.hu

2 Materials and methods

The overall objective of the study is to compare the performance of satellite and drone surveys in case of a particular experimental field. The specifications of the satellite and drone imageries are significantly different. The main differences (Table 1.):

Table 1. Comparison of imagery based on satellite and drone platforms

	Satellite based	Drone based
Spectral bands:	appx 10	appx. 4
Spatial resolution:	meters/pixel level	cm/px level
Temporal resolution:	weekly	per hours
Limiting conditions:	clouds	rain, high wind
Surveying mode:	fully automatic	requires manual interactions

The paper will show the causes of the above differences in the final orthomosaics and vegetation index maps in the case of the given experimental field.

2.1 Study site and experimental field

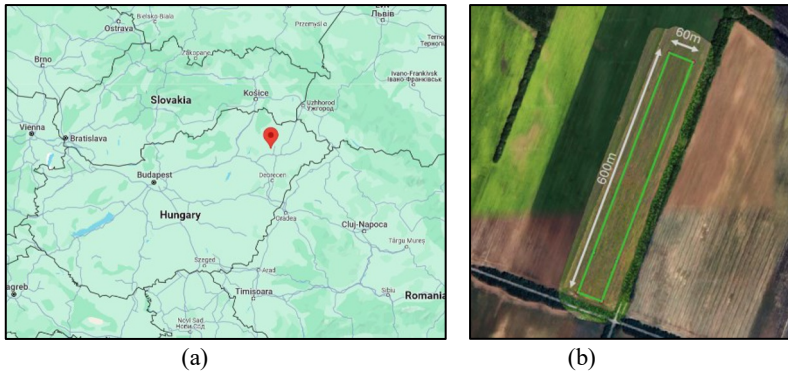


Fig. 1. Location (a) and layout (b) of the experimental site in Hungary

The study was conducted on a crop field located near Nyíregyháza, Hungary (48°00'43.5"N 21°35'35.5"E) in spring of 2024.

The experimental site was a part of a field in an elevation of app. 100m ASL. The difference in the elevation along the field is less than 10m. The site is characterised by acid sandy soil and continental climate with summer droughts making growing conditions difficult.

A rectangular area of 60 m × 60 m was chosen in this field as experimental site for a bilateral project to develop a forecast model for yield productivity. The triticale sown on the experimental site is subject to strict organic farming. In these soils, organic agriculture can be expected to improve soil quality in the long term [9]. No agrotechnical operations or plant protection were applied after sowing on 17 October 2023 at a 200kg/ha seed rate.

2.2 Survey drone

The aerial surveys were conducted with a DJI Mavic 3M Enterprise drone with multispectral camera. (See Figure 2(a))

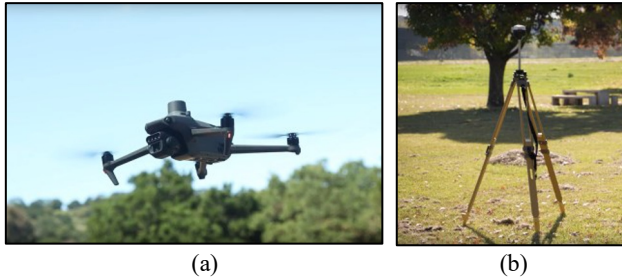


Fig. 2. (a) DJI Mavic 3 Enterprise Multispectral; (b) Emlid RS2+ base station

The drone is optimized for regular surveys with durable and reliable body, propulsion and sensor. Specification of the sensor is shown by Table 2. To improve the spatial precision an Emlid 2RS+ RTK base station was applied (See Figure 2(b)). The position of the station was determined by a 5 min long averaging of the GPS signals improved by RTK correction signal provided the station KEME in a distance of 14 km via the Centipede network [10]. Based on the RTK correction the drone determined a value of the standard deviation of its position of 1 cm or less during the flights.

Table 2. Specifications of the drone sensor. [11]

Image Sensor:	1/2.8-inch CMOS
Effective pixels:	5 MP
Lens FOV:	73.91° (61.2° x 48.10°)
Equivalent focal length:	25 mm
Aperture:	f/2.0
Electronic shutter	1/30~1/12800 s
Focus:	fixed
Green Band (G):	560 ± 16 nm
Red Band (R):	650 ± 16 nm
Red Edge Band (RE):	730 ± 16 nm
Near infrared Band (NIR):	860 ± 26 nm
Gain Range:	1x-32x

2.4 Flight plan

The drone flown the survey missions at 57m AGL altitude to obtain images with a GSD of 25mm/pixel with a gimbal mounted camera in nadir mode (stabilized down looking camera). The drone automatically adjusted the capture settings. Typical values for the multispectral channels in a sunny day:

Image Size	: 2592×1944
Focal length (35mm equivalent)	: 29mm
F-stop	: f/2
ISO	: 100

Shutter speed : 1/640s

The lateral and longitudinal overlap was set to 80% to improve the precision of stitching. Fig. 3. shows a typical pattern of positions images taken from.



Fig. 3. Positions of images on a typical survey mission

The images were processed by the Pix4Dfields v2.6.2 software optimized for agricultural usage. Lacking proper reflectance target, only self-normalizing indices were produced as results.

2.5 Satellite data

The Sentinel-2 project from the Copernicus Programme of the European Space Agency (ESA) consists of two Earth observation satellite acquiring optical images at a spatial resolution of 10 m to 60 m. Revisit time of the pair is app. 5 days. The orbits are Sun-synchronous to optimize the comparability of the images made at different dates.

Various radiometric and atmospheric corrections are applied to deliver bottom of the atmosphere (BOA) reflectance data. The data processed from L1C data with Sen2Cor were utilized in our investigation. Finally, all bands are upsampled to a resolution of 5m and stacked in a raster (.tiff). The proper settings (data selection) were managed by the Pix4Dfields software.

Table 2. Sentinel-2 spectral bands [12]

Band name	Sentinel-2A		Sentinel-2B		Spatial resolution (m)
	Central wavelength (nm)	Bandwidth (nm)	Central wavelength (nm)	Bandwidth (nm)	
1	443,9	27	442,3	45	60
2	496,6	98	492,1	98	10
3	560,0	45	559	46	10
4	664,5	38	665	39	10
5	703,9	19	703,8	20	20
6	740,2	18	739,1	18	20
7	782,5	28	779,7	28	20
8	835,1	145	833	133	10
8a	864,8	33	864	32	20

9	945,0	26	943,2	27	60
10	1373,5	75	1376,9	76	60
11	1613,7	143	1610,4	141	20
12	2202,4	242	2185,7	238	20

3 Results and discussion

3.1 Vegetation indices from drone surveys

Drone survey missions started on 28.03.2024 and were performed with different settings to find the optimal ones. Surveys with the final setting (see Chapter 2.4) were performed weekly from 25.04.2024 to 08.07.2024. Surveys on the following dates (see Table 4.) were selected for the analysis.

Table 4. Surveys involved in analysis.

Date	Local time	Weather
25. April	15:00	clouds
01. May	07:30	clear sky
09. May	07:30	clouds
16. May	07:30	clear sky
22. May	17:30	clouds
06. Juni	08:00	clear sky
13. Juni	07:30	clouds
27. Juni	09:00	clouds
03. July	19:00	clouds

The following vegetation indexes (VI) were calculated based on the multispectral images:

Table 3. Vegetation indices.

Vegetation index	Formula	Ref.
MGRVI	$(G - R)/(G + R)$	Bendig, et al. [13]
GNDVI	$(NIR - G)/(NIR + G)$	Gitelson, Merzlyak [14]
LCI	$(NIR - RedEdge)/(NIR + R)$	Datt, B. [15]
NDRE	$(NIR - RedEdge)/(NIR + RedEdge)$	Gitelson, Merzlyak [14]
SIPI2	$(NIR - G) / (NIR - R)$	Penuelas et al. [16]
NDVI	$(NIR - R)/(NIR + R)$	Rouse et al. [17]

The six VIs for two different dates can be seen in Figure 4. The colour codes for the two dates are the same, thus the images are pairwise quantitatively comparable and are representative for the change in the indices in 24 days. The histograms in the lower right corner of the images are also informative on the distribution of the given index.

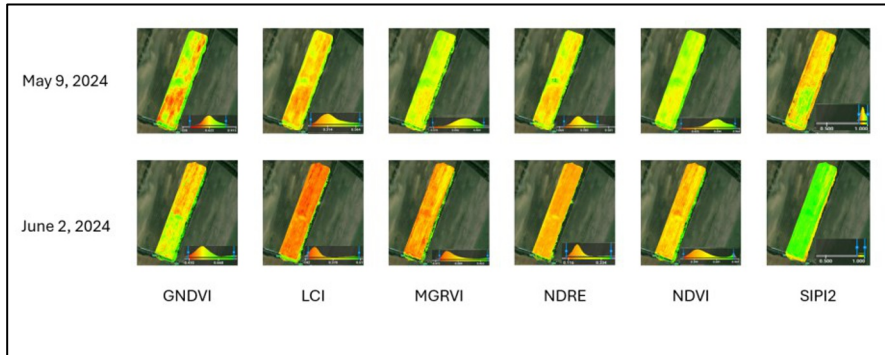


Fig. 4. Vegetation indices for two different dates (May 9. and June 2.)

3.2 Spatial variability in the drone and satellite imagery

The high resolution of the drone images enables a detailed analysis of the structure and topography of the field. For further analysis of drone and satellite performance the Normalized Difference Vegetation Index (NDVI) was selected as the most widely used vegetation index.

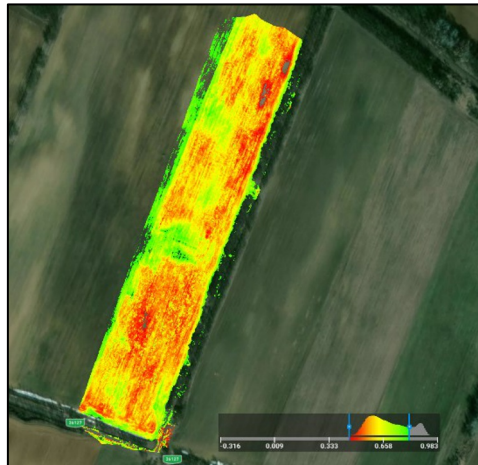


Fig. 5. NDVI map based on drone images on May 22, 2024 showing a significant inhomogeneity

The colour coding of Figure 5 has been limited to the range 0.4 – 0.8 to enhance the inhomogeneity in the map. As a result of the strict organic farming no tramlines can be seen on the picture, but several zones can be identified inside the field caused by weeds and differences in humidity and nutrient content of the soil.

The difference between the drone and satellite NDVI indices can be better demonstrated and numerically evaluated if resampled along a given line. Because of the stretched layout of the field the centreline of the experimental site seemed a reasonable choice. This line can be seen on both NDVI map in Figure 6.

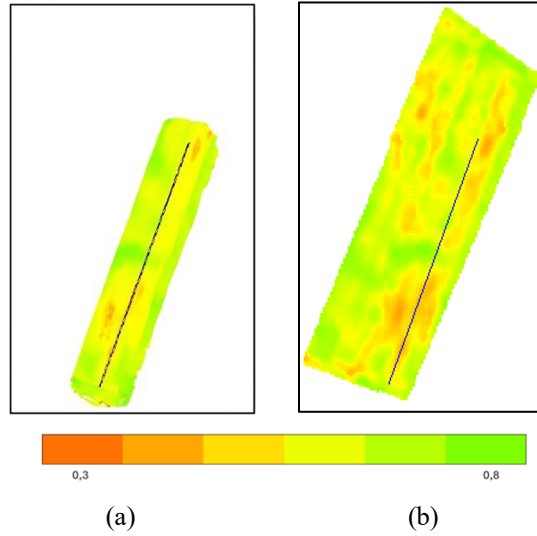


Fig. 6. The same centreline on both NDVI maps: (a) drone survey on 25 April; (b) satellite survey on 30 April. (Colour codes are the same.)

The spatial resolution of a drone NDVI map is significantly better (4 cm/px) than it of the satellite NDVI map (500cm/px). Such a high resolution causes noise hampering the comparison. To remove the noise from the drone NDVI map and improve comparability a moving average filter with a window of 500cm was applied on the drone sample line in Figure 7.

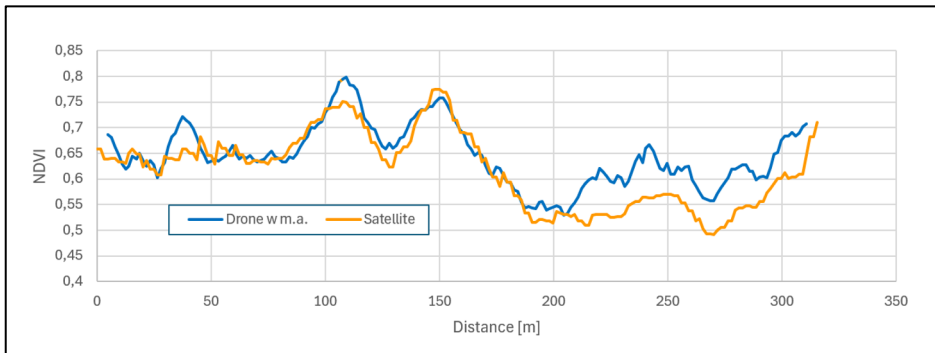


Fig. 7. NDVI indices (Fig. 6.a and Fig. 6.b) along the centreline of the experimental site

The first 200m of the diagram shows a significant similarity in nature and in absolute values, but the rest seems laden with noticeable bias in absolute value, while the nature of the curves are still similar. We suspect that the bias is a function of the soil characteristics, but further research is needed to prove this assumption.

3.3 Temporal variability in the drone and satellite imagery

To compare the time history of the data provided by the drone and the satellites, a smaller spot was chosen. The experimental site consists of five zones originally defined for other tests. Zone 2 was picked for the comparison to decrease the computational demand. The zone

has a limited area of 100m x 140m. Its position can be seen on Figure 8. Its surface seems relative homogenous compared to the rest of the experimental site.

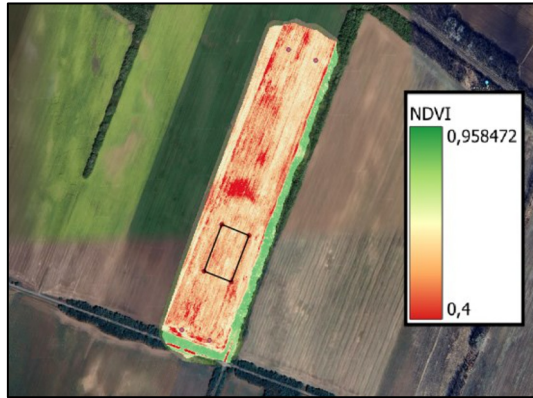


Fig. 8. Location of Zone 2 (solid outline) in the experimental site (NDVI map from drone survey on 3 July 2024)

The image coverage by drone survey of the spot can be seen on Figure 9. and resulted in a GSD of 4cm/px.

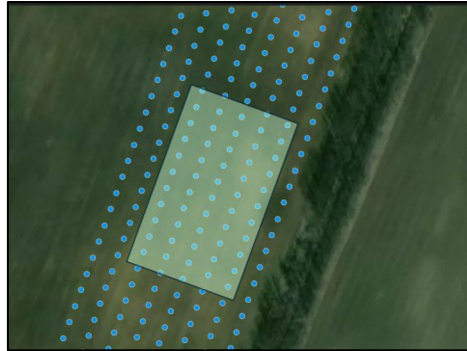


Fig. 9. Location of image shots around and over Zone 2 (drone survey on 3 July 2024)

Time history of the NDVI maps of Zone 2 can be seen on Figure 10. Unfortunately, the date of the satellite and drone images are different, thus the direct comparison of images is a suboptimal approach. In the followings the time histories of the vegetation index NDVI will be compared.

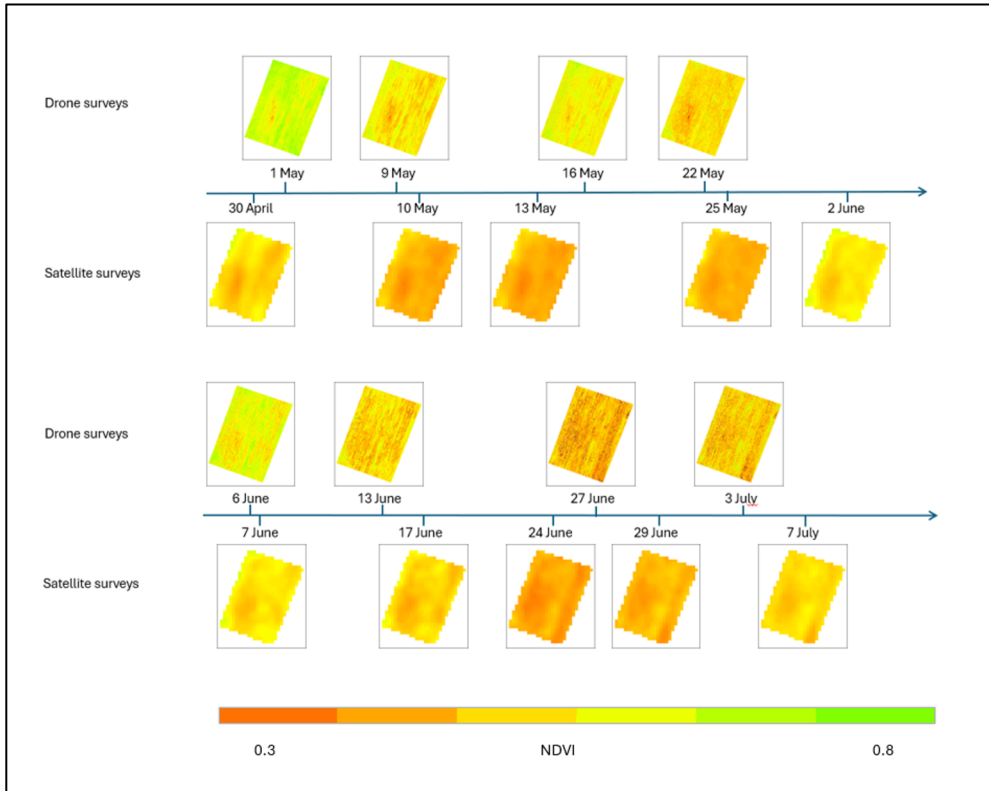


Fig. 10. Time history NDVI maps from drone and satellite surveys involved in the analysis

To better demonstrate the temporal variation of the drone and satellite NDVI indices ten random satellite pixel in Zone 2 were selected.

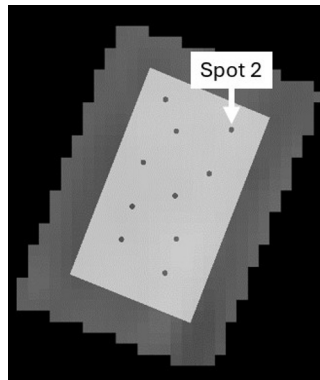


Fig. 11. Location Spot 2 in Zone 2 and nine other similar random spots

First, we selected one of them (namely Spot 2) to compare the time history of NDVI indices measured by the drone and the satellite. One single pixel of the satellite covers a 5m x 5m area. The same area is covered by 125px x 125px in the drone map. To enable the direct comparison a single value of the average NDVI index by the drone was calculated over each spot. The dashed lines in Figure 12 represent the NDVI indices of Spot 2.

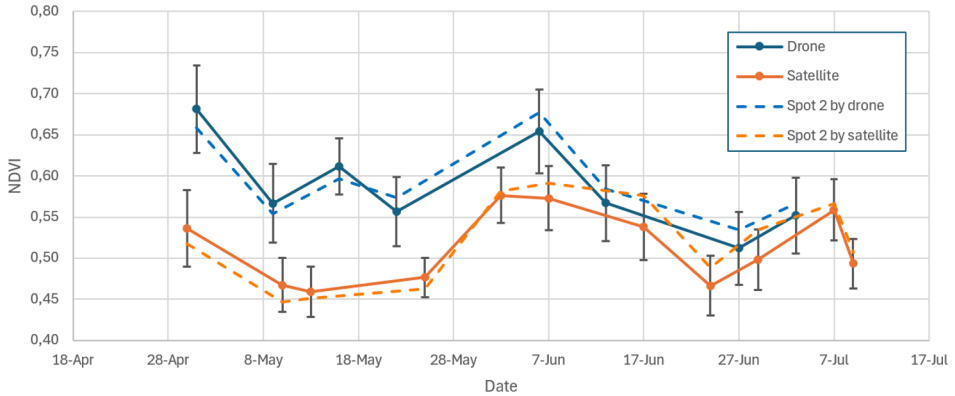


Fig. 12. Time history of NDVI indices of random selected spots in Zone 2

One can observe that the strong correlation between the drone and the satellite imagery shown in Figure 7 is not generally true. Even in the second half of the time the drone and satellite values are close to each other but in the first part of the diagram a gap of approximately 0.1 of NDVI can be seen between the two dotted line. However, the nature of the two curves is still similar.

To specify how representative is a single spot for the zone under the current investigation nine other spots were selected. The solid curves in Figure 12 connect the mean values of the spots in case of both imageries. Thus, these solid curves represent much more reliably the overall NDVI index of the zone in the function of time. Both curves have a wavelike shape as it should be considering the phases of growth stages, but the drone curve indicates some disturbances. The disturbances are significant compared to the standard deviation of the curves and we assumed a systematic error instead of measurement noise. Table 4 contains already the information on the weather during the surveys. Considering this information, it can be assumed, that the sunny weather causes bias in the drone imagery, because there is a noticeable deviation upward from the expected value on the sunny days: 1 May, 16 May, 6 June.

However, even this expected systematic error is neglected, the above-mentioned gap still exists in the first half of the time.

The error bars in the diagram show the standard deviation of the NDVI value specified in the selected spots. The standard deviation do changes with the time in case of both imageries meaning that the inhomogeneity of the crop is a function of times but no tendency can be recognized.

4 Conclusion

Triticale was sown in an experimental field subject of organic farming. The field was observed by Sentinel 2 satellites and by drones in a timespan of 69 days before harvesting with multispectral cameras. Boths platform provides valuable information on the actual state of the crop field by different vegetation indices. The NDVI was chosen to perform a quantitative comparison of the results. The difference between the NDVI provided by the two platform didn't seem homogeneous. The month before harvesting the two platform provided results with less difference than the standard deviation in the spatial distributions. This proved that the drone platform can compensate the lower performance of the low-cost sensor with the lower flight altitude. However, further investigations are required to identify the reason for the higher differences before this period.

References

1. O. Varga, Sz. Szabo, Z. Túri; *Efficiency assessments of GEOBIA in land cover analysis, NE Hungary*. Bulletin of Environmental and Scientific Research. **3**, 1-9. (2014)
2. K.A Sudduth, J.W. Hummel, S.J Birrell; *Sensors for Site-Specific Management*. In *The State of Site Specific Management for Agriculture*; American Society of Agronomy: Madison, WI, USA, 183–210. (1997)
3. R.R. Bosecker; *Sampling Methods in Agriculture*; National Agricultural Statistics Service, US Department of Agriculture: Washington, DC, USA, 1988 Agriculture; American Society of Agronomy: Madison, WI, USA, 183–210 (1997)
4. R. Bogue; *Sensors Key to Advances in Precision Agriculture*. Sens. Rev. 2017, **37**, 1–6 (2017)
5. C.W. Zecha, J. Link, W. Claupein; *Mobile Sensor Platforms: Categorisation and Research Applications in Precision Farming*. J. Sens. Syst **2**, 51–72 (2013)
6. F. Gascon, E. Cadau, O. Colin, B. Hoersch, C. Isola, B.L. Fernández, P. Martimort; *Copernicus Sentinel-2 Mission: Products, Algorithms and Cal/Val*. In Proceedings of the Earth Observing Systems XIX, San Diego, CA, USA, 17–21 August 2014; SPIE: Bellingham, WA, USA, **9218**, 455–463 (2014)
7. M. Drusch, U. Del Bello, S. Carlier, O. Colin, V. Fernandez, F. Gascon, B. Hoersch, C. Isola, P. Laberinti, P. Martimort; *Sentinel-2: ESA's Optical High-Resolution Mission for GMES Operational Services*. Remote Sens. Environ, **120**, 25–36. (2012)
8. M. Piragnolo, G. Lusiani, F. Pirotti; *Comparison of Vegetation Indices from RPAS and Sentinel-2 Imagery for Detecting Permanent Pastures*. Int. Arch. Photogramm. Remote Sens. Spat. Inf. Sci, **42**, 1381–1387 (2018)
9. J. Csabai, B. Braun, M. Tarek, K. I. Oláh; Scientific Bulletin of Uzhhorod University. Series Biology. *Effect of alternative nutrient replenishes on soil quality parameters*. **50-51**, 41-47 (2021)
10. W. Heintz, J. Molina, S. Ladet, L. Larrieu, L. Fabien; *Évaluation des performances de solutions GNSS Real Time Kinematic commerciales et open source pour la géolocalisation des arbres en forêt*. NOV'AE, 2024, 01, 10 (2024)
11. DJI Mavic 3M Enterprise Multispectral User's Manual v1.0; 2022.12; 89 (2022)
12. *Sentinel-2 Products Specification Document REF: S2-PDGS-TAS-DI-PSD 14.9*, 47 (2021)
13. J. Bendig, K. Yu, H. Aasen, A. Bolten, S. Bennertz, J. Broscheit, M.L. Gnyp, G. Bareth; *Combining UAV-Based Plant Height from Crop Surface Models, Visible, and near Infrared Vegetation Indices for Biomass Monitoring in Barley*. Int. J. Appl. Earth Obs. Geoinf. **39**, 79–87 (2015)
14. A.A. Gitelson, M.N. Merzlyak; *Remote Estimation of Chlorophyll Content in Higher Plant Leaves*. Int. J. Remote Sens **18**, 2691–2697 (1997)
15. B. Datt; *Remote Sensing of Water Content in Eucalyptus Leaves* Journal of Plant Physiology **154**, 30-36 (1999)
16. J. Penuelas, F. Baret, I. Filella; *Semi-empirical indices to assess carotenoids/chlorophyll a ratio from leaf spectral reflectance*. Photosynthetica **31**, 221–230 (1995)

17. J.W. Jr. Rouse, R.H. Haas, J.A. Schell, D.W. Deering; *Monitoring Vegetation Systems in the Great Plains with Ertis*. In NASA Special Publication; NASA: Washington, DC, USA **351**, 309 (1974)